

Research article

Genome trees constructed using five different approaches suggest new major bacterial clades

Yuri I Wolf^{†1}, Igor B Rogozin^{†1}, Nick V Grishin^{†2}, Roman L Tatusov¹ and Eugene V Koonin^{*1}

Address: ¹National Center for Biotechnology Information, National Library of Medicine, National Institutes of Health, Bethesda, MD 20894, USA, ²Howard Hughes Medical Institute and Department of Biochemistry, University of Texas Southwestern Medical Center, 5323 Harry Hines Boulevard, Dallas, TX 75390-9050, USA

E-mail: Yuri I Wolf - wolf@ncbi.nlm.nih.gov; Igor B Rogozin - rogozin@ncbi.nlm.nih.gov; Nick V Grishin - grishin@chop.swmed.edu; Roman L Tatusov - tatusov@ncbi.nlm.nih.gov; Eugene V Koonin* - koonin@ncbi.nlm.nih.gov

*Corresponding author †Equal contributors

Published: 23 October 2001

Received: 20 September 2001

BMC Evolutionary Biology 2001, 1:8

Accepted: 23 October 2001

This article is available from: <http://www.biomedcentral.com/1471-2148/1/8>

© 2001 Wolf et al; licensee BioMed Central Ltd. Verbatim copying and redistribution of this article are permitted in any medium for any non-commercial purpose, provided this notice is preserved along with the article's original URL. For commercial use, contact info@biomedcentral.com

Abstract

Background: The availability of multiple complete genome sequences from diverse taxa prompts the development of new phylogenetic approaches, which attempt to incorporate information derived from comparative analysis of complete gene sets or large subsets thereof. Such attempts are particularly relevant because of the major role of horizontal gene transfer and lineage-specific gene loss, at least in the evolution of prokaryotes.

Results: Five largely independent approaches were employed to construct trees for completely sequenced bacterial and archaeal genomes: i) presence-absence of genomes in clusters of orthologous genes; ii) conservation of local gene order (gene pairs) among prokaryotic genomes; iii) parameters of identity distribution for probable orthologs; iv) analysis of concatenated alignments of ribosomal proteins; v) comparison of trees constructed for multiple protein families. All constructed trees support the separation of the two primary prokaryotic domains, bacteria and archaea, as well as some terminal bifurcations within the bacterial and archaeal domains. Beyond these obvious groupings, the trees made with different methods appeared to differ substantially in terms of the relative contributions of phylogenetic relationships and similarities in gene repertoires caused by similar life styles and horizontal gene transfer to the tree topology. The trees based on presence-absence of genomes in orthologous clusters and the trees based on conserved gene pairs appear to be strongly affected by gene loss and horizontal gene transfer. The trees based on identity distributions for orthologs and particularly the tree made of concatenated ribosomal protein sequences seemed to carry a stronger phylogenetic signal. The latter tree supported three potential high-level bacterial clades: i) Chlamydia-Spirochetes, ii) Thermotogales-Aquificales (bacterial hyperthermophiles), and iii) Actinomycetes-Deinococcales-Cyanobacteria. The latter group also appeared to join the low-GC Gram-positive bacteria at a deeper tree node. These new groupings of bacteria were supported by the analysis of alternative topologies in the concatenated ribosomal protein tree using the Kishino-Hasegawa test and by a census of the topologies of 132 individual groups of orthologous proteins. Additionally, the results of this analysis put into question the sister-group relationship between the two major archaeal groups, Euryarchaeota and Crenarchaeota, and suggest instead that Euryarchaeota might be a paraphyletic group with respect to Crenarchaeota.

Conclusions: We conclude that, the extensive horizontal gene flow and lineage-specific gene loss notwithstanding, extension of phylogenetic analysis to the genome scale has the potential of uncovering deep evolutionary relationships between prokaryotic lineages.

Background

The determination of multiple, complete genome sequences of bacteria, archaea and eukaryotes has created the opportunity for a new level of phylogenetic analysis that is based not on a phylogenetic tree for selected molecules, for example, rRNAs, as in traditional molecular phylogenetic studies [1,2], but (ideally) on the entire body of information contained in the genomes. The most straightforward version of this type of analysis, to which we hereinafter refer to as 'genome-tree' building, involves scaling-up the traditional tree-building approach and analyzing the phylogenetic trees for multiple gene families (in principle, all families represented in many genomes), in an attempt to derive a consensus, 'organismal' phylogeny [3–5]. However, because of the wide spread of horizontal gene transfer and lineage-specific gene loss, at least in the prokaryotic world, comparison of trees for different families and consensus derivation may become highly problematic [6,7]. Probably due to all these problems, a pessimistic conclusion has been reached that prokaryotic phylogeny might not be reconstructable from protein sequences, at least with current phylogenetic methods [4].

With the complete genome sequences at hand, it appears natural to seek for alternatives to traditional, alignment-based tree-building in the form of integral characteristics of the evolutionary process. Probably the most obvious of such characteristics is the presence-absence of representatives of the analyzed species in orthologous groups of genes, and recently, at least three groups have employed this approach to build genome trees, primarily for prokaryotes [8–10]. An alternative way to construct a genome tree involves using the mean or median level of similarity among all detectable pairs of orthologs as the measure of the evolutionary distance between species [11]. Yet another possibility involves building species trees by comparing gene orders. This approach had been pioneered in the classical work of Dobzhansky and Sturtevant who used inversions in *Drosophila* chromosomes to construct an evolutionary tree [12]. Subsequently, mathematical methods have been developed to calculate rearrangement distances between genomes, and, using these, phylogenetic trees have been built for certain small genomes, such as plant mitochondria and herpesviruses [13,14]. These approaches, however, are applicable only to genomes that show significant conservation of global gene order, which is manifestly not the case among prokaryotes [15–17]. Even relatively close species such as, for example, *Escherichia coli* and *Haemophilus influenzae*, two species of the γ -subdivision of Proteobacteria, retain very little conservation of gene order beyond the operon level (typically, two-to-four genes in a row), and essentially none is detectable among evolutionarily distant bacteria and archaea [15,16,18]. Very

few operons, primarily those coding for physically interacting subunits of multiprotein complexes such as certain ribosomal proteins or RNA-polymerase subunits, are conserved across a wide range of prokaryotic lineages [15,16]. On the other hand, pairwise comparisons of even distantly related prokaryotic genomes reveal considerable number of shared (predicted) operons, which creates an opportunity for a meaningful comparative analysis [19][20,21].

The critical issue with all these approaches to genome tree building is to what extent each of them reflects phylogeny and to what extent they are affected by other evolutionary processes, such as lineage-specific gene loss and horizontal gene transfer. Comparative analyses have strongly suggested that these phenomena make major contributions to genome evolution, at least in prokaryotes [7,22–25]. These phenomena have the potential to severely affecting phylogenetic tree topology, particularly when similar sets of genes are lost indifferent lineages because of similar environmental pressures, or when a preferential trend of horizontal gene flow exists between different lineages. The possibility even has been discussed that the amount of lateral gene exchange is such that it invalidates the very principle of representing the evolution of species as a tree; instead, the only adequate representation of evolutionary history could be a complex network [6][25]. Genome-trees seem to be the last resort for the species tree concept. Unless phylogenetic signal can be revealed by at least some approaches based on genome-wide comparisons, the conclusion seems imminent that this concept should be abandoned and replaced by a more complex representation of evolution.

Here, we compare the topologies produced with five, largely independent approaches to genome-tree building: i) presence-absence of genomes in Clusters of Orthologous Groups of proteins (COGs); ii) conservation of local gene order (pairs of adjacent genes) among prokaryotic genomes; iii) distribution of percent identity between apparent orthologs; iv) sequence conservation in concatenated alignments of ribosomal proteins; v) comparative analysis of multiple trees reconstructed for representative protein families. We find that, while the presence-absence approach is most heavily affected by gene loss and horizontal transfer, the other four methods reveal stronger phylogenetic signals. Although the topologies of the trees constructed with different approaches were only partially compatible, three previously unnoticed high-level clades among bacteria were revealed with notable consistency. We suggest that, in spite of all the complexity brought about by horizontal gene transfer and lineage-specific gene loss, these groups reflect certain evolutionary reality, i.e. the trajectory of evolution for a relatively stable gene core. It appears that this is the

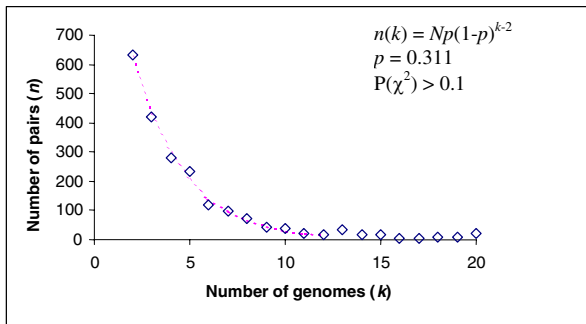


Figure 1
Distribution of conserved gene pairs among 31 clades of prokaryotes. Closely related genomes: *E. coli*-*Buchnera* sp., *H. influenzae*-*P. mutocida*, *C. trachomatis*-*C. pneumoniae*, *P. horikoshii*-*P. abyssi*, *M. genitalium*-*M. pneumoniae*-*U. urealyticum*, *H. pylori* - *C. jejuni*, *T. acidophilum*-*T. volcanium*, were treated as a single clade. *N* is the total number of conserved gene pairs.

only meaningful way to treat the notion of a species tree: as the history of a relatively large ensemble of genes, not a comprehensive representation of the history of entire genomes.

Results

New criteria for genome-tree construction

To our knowledge, conserved gene pairs and distributions of identity level between orthologs have not been used previously as the basis for phylogenetic tree construction. Therefore we start by describing the relevant results of prokaryotic genome comparison in somewhat greater detail.

Conserved gene pairs in prokaryotic genomes

The results of the present analysis of conserved gene pairs are consistent with the notion of the fluidity of prokaryotic gene order caused by extensive recombination. Only 17 invariant genes pairs were detected, all of which consists of genes for ribosomal proteins and RNA polymerase subunits. The remaining 4586 gene pairs were missing in at least one genome. The number of gene pairs represented in three, four and a greater number of genomes decayed rapidly, with highly conserved pairs forming the tail of the distribution (Fig. 1). The 95% quantile of this distribution (excluding the highly conserved pairs) was found to fit the geometric model with a high statistical significance (Fig. 1). This is compatible with random, independent loss of gene pairs during evolution suggesting that, with the caveat of horizontal transfer, the number of gene pairs shared by three genomes could reflect the evolutionary distance between them.

The number of conserved gene pairs present in individual prokaryotic genomes varied from 208 for *M. genitalium* to 2314 for *P. aeruginosa* (Table 1). Analysis of the co-occurrence of gene pairs among the prokaryotic genomes shows high values of the Jaquard coefficient, which reflect partial conservation of gene order (see legend to Table 1), for closely related species, for example, 0.32 for *E. coli* and *H. influenzae* and 0.35 for *M. thermoautotrophicum* and *M. jannaschi* (Table 1). The value of this coefficient varied from 0.16 to 0.66, with a mean of 0.26, for archaea, and from 0.04 to 0.87, with a mean of 0.16, for bacteria. In contrast, for archaeal-bacterial comparisons, the values varied from 0.04 to 0.18, with the average of 0.08 (Table 1). These observations appear to indicate that the distribution of conserved gene pairs among prokaryotic genomes carries a phylogenetic signal.

Distributions of identity percentage between probable orthologs from complete prokaryotic genomes

Figure 2 shows a sampling of the distributions of identity percentage between pairs of apparent orthologs identified as reciprocal best hits from a range of genome pairs separated by varying phylogenetic distances. Most of the distributions are clearly unimodal, and the distributions for pairs of phylogenetically distant genomes, such as those from different major bacterial lineages or bacteria versus archaea, have their modes within a relatively narrow range around 33% identity (Figure 2).

The use of reciprocal best hits is a conservative way to identify the set of probable orthologs between pairs of genomes because some of the orthologs are missed due to complex relationships between groups of paralogs. Nevertheless, all genome-to-genome comparisons included at least 100 (for the smallest genomes such as the mycoplasmas), and typically, a considerably greater number of protein pairs ([11] and data not shown). This suggests that parameters of the distributions of the similarity level between probable orthologs identified in this fashion could potentially serve as useful measures of the evolutionary distance between genomes.

Genome trees constructed with three different approaches

Genome trees were generated using the approaches described under Material and Methods. All the trees showed a clear separation of the two major prokaryotic domains, Bacteria and Archaea (Fig. 3,4,5). Several terminal bifurcations that reflect clustering of relatively close species, such as three mycoplasmas (*M. genitalium*, *M. pneumoniae* and *U. urealyticum*), two spirochetes (*B. burgdorferi* and *T. pallidum*), and *H. pylori* and *C. jejuni*, are also reproduced in all trees (Fig. 3,4,5). This retention of both the deepest and the terminal branchings shows that all types of data used for tree con-

Table 1: Shared gene pairs in prokaryotic genomes.

	Aer	Sus	Arf	Pyh	Pya	Mej	Met	Has	Tha	Thv	Esc	Vic	Hai	Pam	Buc	Psa	Xyf	Ne m	Cac	Mel	Rip	He p	Caj	Bas	Bah	Lal	Sta	Stp	Myp	Myg	Urn	Myt	SyP	Der	Bob	Trp	Chp	Cht	Aqa	Thm
Aepre	495	298	263	207	241	123	172	238	212	227	198	61	102	112	138	209	93	92	146	219	53	87	116	190	200	128	149	96	55	54	51	164	82	172	66	64	63	65	75	148
Sulso	30	775	333	242	775	159	211	795	353	352	795	87	124	145	186	333	137	109	234	332	70	106	152	310	313	194	233	126	53	52	46	281	107	241	60	54	63	63	91	219
Arcfu	26	27	756	260	302	205	277	331	281	293	273	64	130	162	223	327	125	109	218	300	68	115	164	250	267	157	188	130	49	46	57	196	134	222	84	74	65	67	111	190
Pyrho	26	23	26	493	434	170	221	219	195	207	178	56	96	105	139	170	95	84	112	167	44	77	100	167	172	103	132	91	40	40	44	120	84	151	74	74	53	51	68	162
Pyrab	28	25	28	66	595	205	250	252	221	237	225	66	116	130	179	220	119	87	140	205	48	96	140	217	215	145	178	99	51	48	53	141	99	179	78	72	62	60	68	196
Metja	17	16	22	25	27	347	225	147	134	142	108	43	63	75	85	108	68	54	79	105	35	52	81	99	94	71	88	62	35	33	37	86	74	96	44	46	39	34	62	106
Metth	20	19	28	28	29	35	507	224	180	196	162	65	89	108	141	162	110	77	115	147	50	74	104	162	159	120	136	81	42	40	43	132	113	136	58	62	49	49	78	173
Halsp	24	24	29	22	24	16	22	705	270	274	252	75	135	159	220	335	129	123	245	334	74	112	155	284	284	180	222	142	70	63	65	236	142	260	91	84	67	68	86	168
Theac	23	34	25	21	22	16	19	25	611	494	238	67	102	108	156	285	102	98	198	273	68	103	122	234	229	147	181	102	46	45	40	213	95	197	53	57	60	62	75	147
Thevo	25	33	27	22	24	17	21	26	622	243	69	99	109	148	283	111	104	188	272	73	102	123	222	224	144	177	100	47	47	40	219	100	202	54	54	60	60	80	147	
Escco	8	12	11	7	9	4	7	10	10	1953	415	700	826	1178	1368	634	491	734	1000	191	263	378	783	721	452	566	303	136	123	107	544	282	478	198	173	165	159	209	409	
Vibch	6	7	5	6	6	5	7	6	6	447	241	274	362	346	262	216	196	214	113	122	145	213	206	125	177	91	84	81	73	186	83	134	112	100	99	97	101	176		
Haein	8	8	8	7	8	5	6	9	7	37	22	875	684	648	632	358	335	343	418	135	172	231	359	347	273	331	216	105	99	108	252	136	236	140	116	132	126	113	241	
Paspu	7	8	9	7	8	5	7	9	6	6	32	22	54	1058	794	738	415	370	401	482	140	189	277	423	418	286	365	222	110	100	104	268	172	264	145	135	142	138	132	278
Bucsp	6	8	10	6	8	4	6	10	7	6	48	20	34	41	1650	1256	594	467	648	780	180	231	345	677	648	372	490	286	126	113	110	420	271	403	202	174	166	162	192	372
Pseae	8	12	11	6	8	4	6	12	10	10	47	14	24	28	46	2314	704	537	997	1297	224	268	397	926	849	447	589	330	135	126	122	691	380	624	220	184	181	179	248	419
Xylfa	7	9	8	7	8	5	8	8	7	7	28	24	25	27	30	877	345	461	471	154	175	217	375	355	227	297	162	84	82	85	312	178	271	134	118	125	128	154	239	
Neime	8	7	8	7	7	5	6	9	8	8	22	23	26	76	24	21	27	703	332	383	151	178	238	306	300	193	233	157	85	85	79	258	138	225	105	117	123	120	128	192
Caucr	8	11	11	6	7	4	6	13	10	10	27	11	17	19	26	36	25	18	1417	1020	206	196	289	638	605	311	432	228	96	92	88	561	295	456	149	139	135	128	186	302
Meslo	9	13	12	7	8	4	6	14	12	11	34	9	17	19	27	43	20	16	43	1937	225	220	337	850	792	430	527	300	103	103	107	691	369	582	177	161	164	157	208	400
Ricpr	6	6	6	5	5	5	6	7	7	8	9	17	12	11	10	9	14	17	13	11	319	91	116	175	165	108	138	99	71	70	63	149	100	139	82	71	81	82	86	109
Helpy	10	9	10	9	10	7	8	11	11	11	12	16	15	14	12	10	15	19	12	10	14	407	250	203	217	147	183	113	76	73	88	172	100	171	110	105	90	89	131	162
Camje	11	12	13	10	13	9	10	13	11	11	17	16	18	20	18	15	17	22	16	15	14	33	592	329	312	202	240	134	81	77	80	239	177	232	113	118	100	94	150	222
Bacsu	9	13	11	8	10	4	7	13	10	10	26	10	15	17	24	29	16	14	25	29	9	10	16	1755	1234	615	931	486	178	175	164	621	284	530	223	197	162	154	186	473
Bacha	10	14	12	8	10	4	7	13	11	10	25	10	15	18	24	27	16	14	24	28	9	11	16	56	1646	575	869	460	173	166	166	594	282	522	213	193	158	149	191	491
Lacla	9	12	10	7	10	5	9	12	10	10	18	10	17	16	16	15	14	13	15	17	9	12	15	29	28	927	534	473	150	137	124	363	158	314	129	114	111	107	115	325
Staa	9	12	10	8	10	5	8	12	10	10	21	11	18	18	20	19	16	13	19	19	9	12	14	44	42	32	1254	434	182	169	169	480	215	395	170	140	160	146	141	384
Strpy	8	9	9	8	8	6	7	11	8	8	12	8	15	14	13	12	11	12	11	12	10	11	11	24	24	40	716	150	137	128	246	128	240	138	120	110	106	92	235	
Mycpn	8	5	5	5	6	6	6	8	5	5	6	14	10	9	7	5	8	10	6	4	14	13	10	9	10	14	14	18	228	203	138	119	63	100	95	74	66	66	61	110
Mycge	8	5	5	6	6	6	5	7	5	6	6	14	10	8	6	5	8	10	6	5	15	13	10	9	9	13	13	17	87	208	133	118	62	97	93	72	67	67	62	109
Ureur	7	4	6	6	7	7	6	7	5	5	5	12	11	9	6	5	8	9	5	5	13	16	11	9	9	12	13	16	47	48	201	117	62	100	89	75	65	64	57	113
Myctu	10	16	11	7	8	5	8	14	13	13	20	12	13	13	17	24	17	15	27	28	10	12	15	26	26	20	24	14	9	9	9	1188	255	444	125	127	133	132	163	289
SynPC	7	8	10	8	8	8	11	12	8	8	12	8	10	11	13	14	13	11	16	16	11	10	17	13	14	11	12	10	8	8	8	16	620	255	76	83	72	69	140	165
Deira	13	15	14	11	12	7	9	18	13	14	19	10	14	14	17	23	16	15	23	24	11	13	17	23	24	19	21	16	8	8	9	25	18	998	136	118	124	122	156	269
Borbu	8	5	8	9	9	7	7	9	6	6	9	17	13	11	11	9	12	11	9	8	14	17	14	12	12	11	12	15	20	21	20	9	8	11	322	191	104	100	87	152
Trepa	8	5	7	10	8	7	8	9	6	6	8	15	10	10	9	7	11	13	8	7	12	17	15	10	10	10	9	13	15	16	17	9	9	9	43	312	94	94	93	161
Chlpr	9	6	6	7	7	6	6	7	7	7	8	16	13	12	9	7	12	14	8	8	16	15	13	8	9	10	11	12	15	16	16	10	8	10	21	19	267	245	75	123
Chltr	9	6	7	7	7	5	6	7	7	7	7	15	12	11	9	7	12	14	8	7	16	15	12	8	8	9	10	12	15	16	16	10	8	10	20	19	87	258	73	121
Aquae	8	8	10	7	7	8	9	8	7	8	9	12	9	9	10	9	13	12	11	9	12	18	17	9	10	9	9	8	10	10	9	11	15	12	13	14	12	11	432	

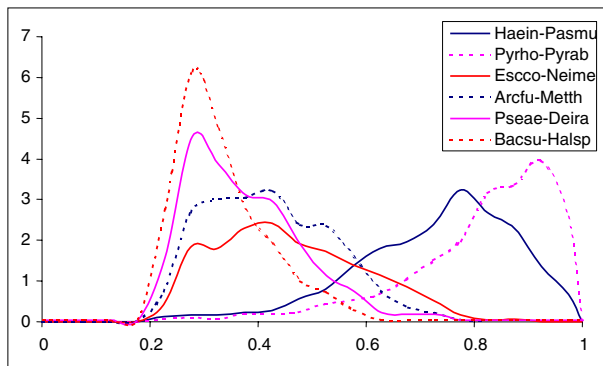


Figure 2
Distribution of identity percentage between probable orthologs in genome pairs. The distributions are for the sets of probable orthologs detected with an e-value cut-off of 0.001. For species name abbreviations, see Materials and Methods.

struction contained at least a crude phylogenetic signal. However, beyond these obvious aspects of topology, and in particular with respect to clustering of distantly related bacteria and archaea, the trees produced with different approaches showed significant differences, which appear to reflect the relative contributions of phenotypic and phylogenetic signals. A quantitative comparison of the tree topologies using the symmetric distance method showed that the presence-absence tree was most different from the trees made by the other methods (Table 2).

Presence-absence of genomes in COGs

The topology of the parsimony tree built using this criterion appears to reflect primarily the phenotypes of the respective organisms (Fig. 3). This is most clearly manifest in the two major bacterial clusters that appear in this tree, each with a strong bootstrap support:

- i) bacteria with large genomes, namely *E. coli*, *B. subtilis*, *Synechocystis sp.*, *Deinococcus radiodurans* and *Mycobacterium tuberculosis*, and free-living bacteria with small genomes, *A. aeolicus* and *T. maritima*
- ii) parasites with small genomes (mycoplasmas, spirochetes, chlamydia and rickettsia)

Parasites with moderate-sized genomes (*H. influenzae*, *N. meningitidis*, and *P. multocida*; *H. pylori* and *C. jejuni*) formed two distinct groups. Thus, well-established phylogenetic relationships between free-living and parasitic bacteria, such as those within the Proteobacteria (*E. coli*-*H. influenzae*-*P. multocida*-*N. meningitidis*) and

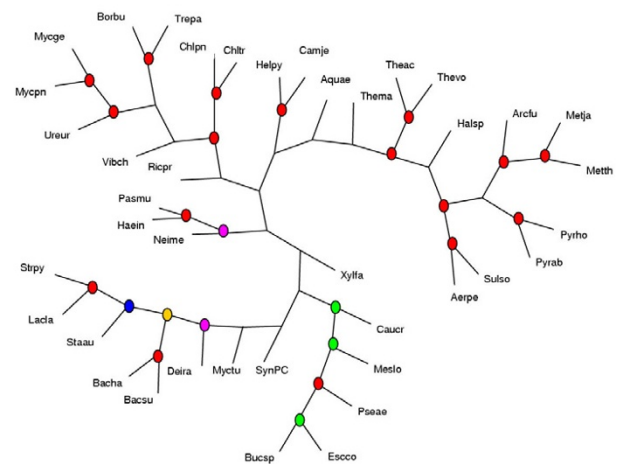


Figure 3
Maximum parsimony tree (Dollo parsimony) based on absence-presence of genomes in orthologous gene sets. The tree is unrooted. The circles indicate the level of bootstrap support, with the following color coding: red: 90–100%, yellow: 80–90%, green: 70–80%, blue: 60–70%, magenta: 40–60%. The nodes with <40% support are unmarked.

within low-GC Gram-positive bacteria (*B. subtilis*-*mycoplasmas*), are not reflected accurately in this tree topology. The two free-living bacteria with small genomes, the hyperthermophiles *A. aeolicus* and *T. maritima*, did not join either the free-living or the parasitic bacterial cluster, despite their small number of genes similar to that in bacterial parasites (Fig. 3). That these bacteria do not group with the parasites despite similar genome sizes, suggests that it is not the number of genes per se, but rather the degree of genome degradation and the loss of coherent sets of genes that affect the topology of the presence-absence tree. The inclusion of the parasites *M. tuberculosis* and *Pseudomonas aeruginosa* in the cluster of bacteria with large genomes probably reflects the recent origin of parasitism in these lineages. It is further notable that, in this tree, the two representative of Crenarchaeota (*A. pernix* and *S. solfataricus*) do not comprise a sister group of the Euryarchaeota (the remaining archaeal species), but rather form a branch within the Euryarchaeal cluster (see discussion below).

In previous studies that employed similar approaches to genome-tree building, phylogenetically reasonable clades were observed after a simple omission of parasitic species [8,9]. Such an operation could be applied to the tree shown in Fig. 3, indeed resulting in the correct recovery of the proteobacterial and Gram-positive bacteri-

Table 2: Symmetric distances between genome-trees constructed with different methods.

	Gene presence-absence Symmetric distance ^a	Conserved gene pairs	Identity distributions
Gene presence-absence			
Conserved gene pairs	52		
Identity distributions	54	44	
Concatenated ribosomal proteins	56	44	38

^aNumber of different partitions of the total of 74 partitions.

number of shared gene pairs was detected during the present analysis (Table 1). Artifacts of tree construction could also contribute to these associations. In contrast, the spirochete-chlamydia clade might reflect a deep phylogenetic relationship (see discussion below).

Parameters of percent identity distributions between orthologs

Different characteristics of the distributions of percent identity between the probable orthologs, such as the mean, the median, the mode and various quantiles, were used to calculate distances between genomes and construct phylogenetic trees. Trees built with different cut-off values for symmetrical best hits, four different formulas for the evolutionary distance calculation (see Materials and Methods) and different parameters of the distributions showed essentially the same topology, with strong bootstrap support for most of the clades (Fig. 5 and data not shown). The complete proteobacterial and Gram-positive bacterial clusters were recovered in this tree as well as the unexpected grouping of chlamydia with spirochete noticed above in the tree based on conserved gene pairs (Fig. 4,5). Also similarly to the previous two trees, the Crenarchaea grouped with *Thermoplasma* within the archaeal part of the tree. Beyond these groupings, the tree appeared conservative in the sense that the unassigned bacterial species formed separate branches near the root of the bacterial subtree. The closest to the root were the two hyperthermophilic species, *A. aeolicus* and *T. maritima*, which is compatible with the standard view of their phylogenetic position [1,26].

Alignment-based approaches to the construction of a species tree

The above three approaches involve construction of genome trees "par excellence", i.e. based on integral characteristics of genomes (or, more precisely, gene sets) that are not directly related to more traditional, alignment-based measures, which are usually employed for calculating evolutionary distances or for parsimony analysis. These genome tree raise several interesting phylogenetic

questions, for example, do spirochetes and chlamydia indeed share a common ancestor, and are Euryarchaeota, in fact, a paraphyletic group with respect to the Crenarchaeota. However, the reliability of the conclusions drawn from the topology of these trees remains uncertain. Therefore we decided to complement these genome-oriented approaches with more traditional ones applied on a large scale.

Concatenated alignments of ribosomal proteins

The alignments of the 32 ribosomal proteins conserved in all bacterial and archaeal species were concatenated head-to-tail and treated as a single alignment containing 4821 columns. The underlying assumption is that the genes coding for ribosomal proteins that function as components of a large macromolecular complex are unlikely to undergo horizontal transfer, which tends to confound comparisons of the tree topologies for other protein families and would invalidate the concatenation approach. The resulting maximum-likelihood tree contains the complete proteobacterial and Gram-positive bacterial clusters as well as the spirochete-chlamydia cluster noticed in the genome-trees. In addition to the spirochetes-chlamydia clade, the following non-trivial affinities were detected with strong bootstrap support: i) a cluster of the two hyperthermophiles, *A. aeolicus* and *T. maritima*, ii) a cluster including *D. radiodurans*, *Synechocystis*, and *M. tuberculosis*, which, at a deeper level, joined the Gram-positive bacterial branch (Fig. 6). Similar tree topologies were obtained when the ribosomal protein data were analyzed using the neighbor-joining method and when bacterial phylogeny was analyzed separately by using a concatenated alignments of 51 ribosomal proteins shared by all bacteria (data not shown). Notably, in the quantitative comparison of tree topologies, the tree made of concatenated ribosomal protein alignments showed the closest similarity to the genome-tree based on the distributions of percent identity between orthologs (Table 2).

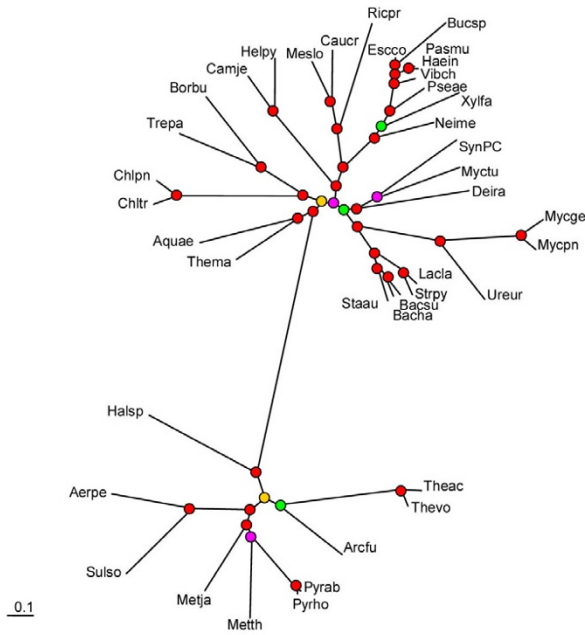


Figure 6
Maximum-likelihood tree produced from concatenated alignments of the universal subset of ribosomal proteins. The designations are as in Fig. 3.

The reliability of the observed non-trivial groupings was further examined by using a maximum likelihood approach (the Kishino-Hasegawa test). For each clade (usually, species) forming the group to be tested, trees with alternative topologies were manually constructed by joining the clade in question to every other major group in the tree. For example, to assess the support for the spirochetes-chlamydia grouping, spirochetes were placed, sequentially, with *Thermotoga*, *Aquifex*, the *Thermotoga-Aquifex* branch, ϵ -proteobacteria, the $\alpha\beta\gamma$ -proteobacterial branch, Proteobacteria, the *Deinococcus-Synechocystis-Mycobacterium* cluster, the low G+C Gram-positive cluster, the branch that unites the latter two clusters, and between bacteria and archaea (to the bacterial root). The same alternatives were tested for chlamydia. Alternative topologies were compared either directly, using the ProtML program, or were subjected to local rearrangement first. In cases when the topology did not revert to the original one, the final, "optimized" topology was used for the comparison. These tests showed high stability of the *Thermotoga-Aquifex* and *Deinococcus-Synechocystis-Mycobacterium* groupings (no competing topologies with likelihood within 1 SD unit from the original; Fig. 7,8, Table 3,4,5,6). The affinity of the *Deinococcus-Synechocystis-Mycobacterium* with Gram-positive bacteria also was supported, although an alternative topology, with this cluster joining Proteobac-

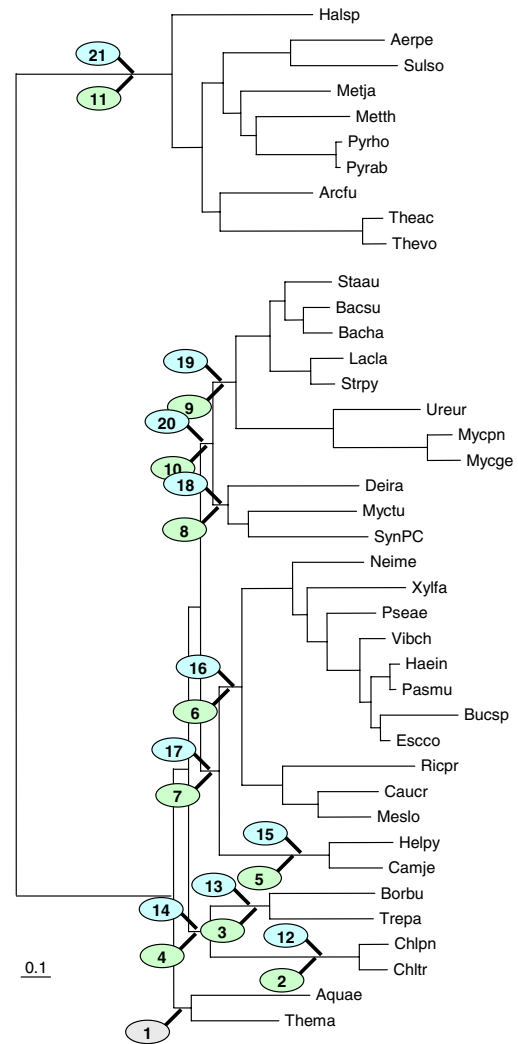


Figure 7
The Kishino-Hasegawa test for the *Aquifex-Thermotoga* clade. "1" indicates the original position of the tested clade in the concatenated ribosomal proteins tree (Fig. 6). The remaining numbers show the alternative positions tested for each of these species (in green ovals for *Aquifex* and blue for *Thermotoga*). For the likelihood values and RELL bootstrap values for each of the corresponding topologies, see Table 3A.

teria could not be ruled out (Fig. 9, Table 7). Assessment of the spirochete-chlamydia grouping revealed two competing topologies, albeit unusual ones. Specifically, moving ϵ -proteobacteria from the proteobacterial branch to the spirochete branch or, alternatively, moving spirochetes with ϵ -p roteobacteria and simultaneously moving chlamydia to the bacterial root results in statistically

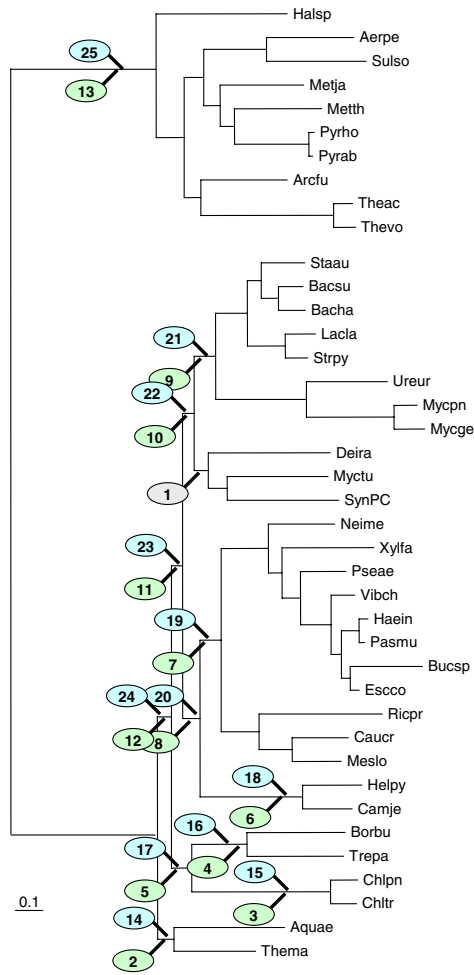


Figure 8
The Kishino-Hasegawa test for the *Deinococcus-Mycobacterium-Synechocystis* clade. The identical scheme of producing alternative topologies was used for each of the three species. For example for *Deinococcus* (see Table 4) the green ovals (## 2 to 13) indicate alternative placements of *Deinococcus* with *Mycobacterium* and *Synechocystis* occupying the original position and the blue ovals (## 14 to 25) indicate alternative placements of the *Mycobacterium-Synechocystis* pair with *Deinococcus* left in the original position. The same was done with *Mycobacterium* versus *Deinococcus-Synechocystis* pair (Table 5) and *Synechocystis* versus *Deinococcus-Mycobacterium* pair (Table 6).

acceptable topologies (Fig. 10; Table 8,9). Also, a minor rearrangement of the topology within the euryarchaeal branch allowed for a reasonable alternative to the topology in Fig. 8 (euryarchaeal paraphyly), with the Crenarchaea-Euryarchaea radiation at the archaeal root (Fig. 11, Table 10).

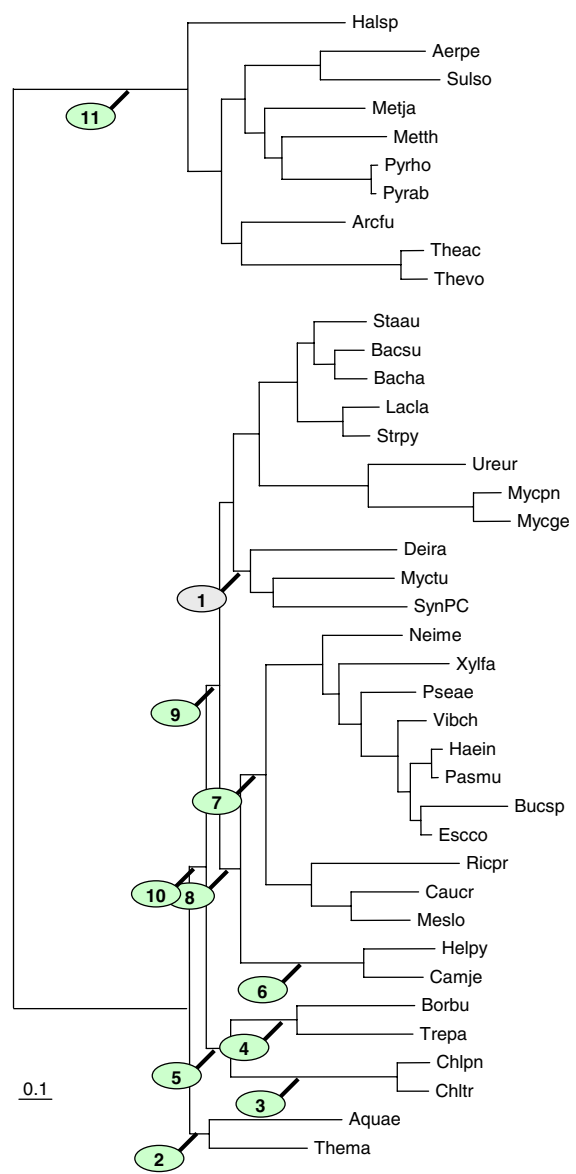


Figure 9
The Kishino-Hasegawa test for the unification of the *Deinococcus-Mycobacterium-Synechocystis* clade with Gram-positive bacteria. See Table 7.

A census of protein families

Another approach to the "species tree" problem involves analysis of phylogenetic trees for as many individual protein families as possible, in an attempt to identify a prevailing topology or at least common phylogenetic patterns. A survey of the COG data set identified 132 COGs, each of which included a large number of bacterial

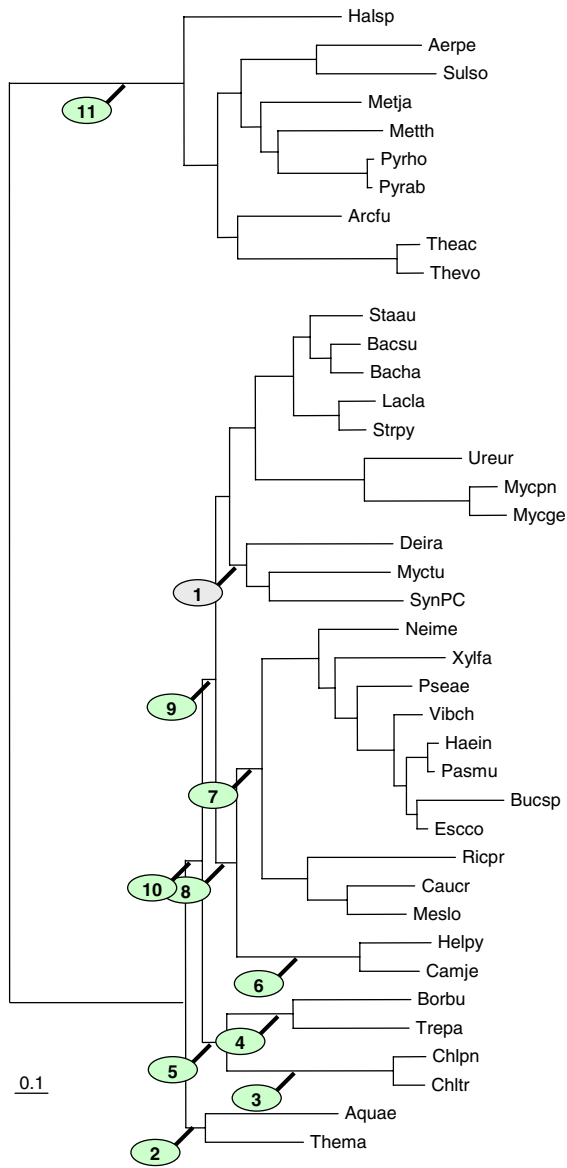


Figure 10
The Kishino-Hasegawa test for the Spirochete-Chlamydia clade. Green ovals: chlamydia, blue ovals: spirochetes. See Table 8.

and archaeal species, but no or few paralogs and thus appeared to be amenable to a large-scale phylogenetic analysis (Table 11). Maximum-likelihood trees were constructed for each of these COGs, and a breakdown of nearest neighbors was derived for species and groups involved in each of the non-trivial or questionable branchings discussed above (Crenarchaea, Thermotoga,

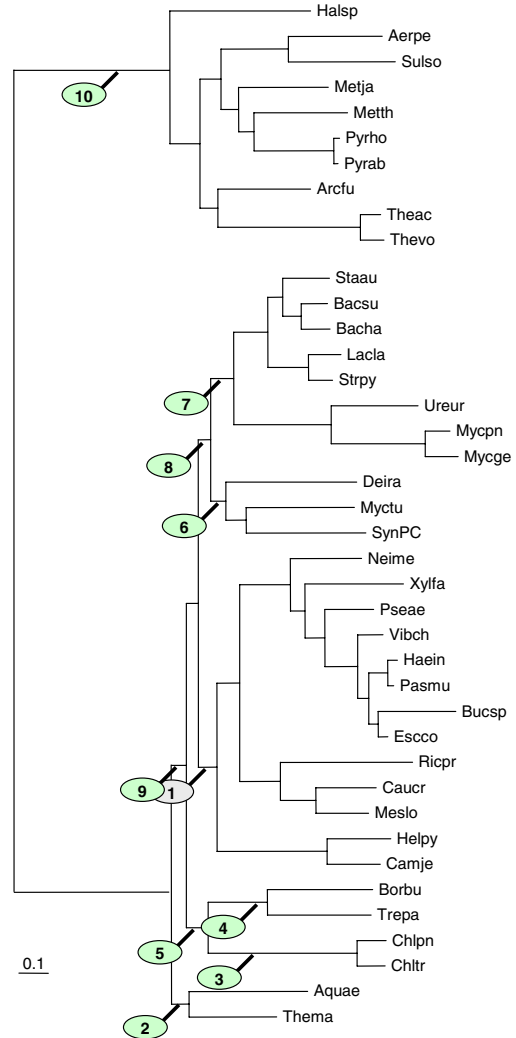


Figure 11
The Kishino-Hasegawa test for the unification of ϵ -proteobacteria with the rest of Proteobacteria. See Table 9.

Aquifex, Deinococcus, Mycobacterium, Synechocystis, spirochetes, chlamydia, and ϵ -proteobacteria). In each case, a wide spread of topologies was observed, but the grouping that is observed in the concatenated ribosomal proteins tree was encountered most often, although, for example, for the spirochete-chlamydia cluster, the lead over other topologies was slim (Fig. 13,14,15).

Discussion and Conclusions

The trees constructed with each of the four approaches employed here reflect both the phylogenetic signal and the phenotypic (life style) similarities or differences between organisms, but the relative contributions of these

Table 3: Testing non-trivial groupings from the concatenated ribosomal protein tree with the Kishino-Hasegawa test^a

(A)
Aquifex-Thermotoga

#	Likelihood	ΔL^b	$\sigma \Delta L^c$	RELL-BP ^d
1	-242983.7	best	N/A	0.9251
2	-243174.6	-190.9	38.5	0.0000
3	-243185.0	-201.3	38.0	0.0000
4	-243146.1	-162.5	32.1	0.0000
5	-243267.6	-283.9	49.0	0.0000
6	-243293.3	-309.7	49.0	0.0000
7	-243218.8	-235.2	41.8	0.0000
8	-243301.0	-317.3	45.7	0.0000
9	-243315.4	-331.8	45.0	0.0000
10	-243242.8	-259.1	40.0	0.0000
11	-243005.7	-22.0	12.2	0.0227
12	-243196.1	-212.4	39.2	0.0000
13	-243201.5	-217.9	38.8	0.0000
14	-243157.9	-174.3	32.2	0.0000
15	-243318.8	-335.1	49.8	0.0000
16	-243355.8	-372.1	48.3	0.0000
17	-243247.1	-263.4	42.1	0.0000
18	-243236.5	-252.8	51.2	0.0000
19	-243232.0	-248.3	51.1	0.0000
20	-243207.0	-223.3	45.0	0.0000
21	-243002.6	-19.0	12.8	0.0522

Table 4:

(B)
Deinococcus radiodurans

#	Likelihood	ΔL	$\sigma \Delta L$	RELL-BP
1	-242983.7	best	N/A	0.8239
2	-243091.1	-107.4	40.8	0.0002
3	-243122.6	-138.9	43.0	0.0000
4	-243135.8	-152.1	43.1	0.0000
5	-243088.1	-104.5	36.3	0.0000
6	-243037.3	-53.7	41.0	0.0775
7	-243064.0	-80.4	40.2	0.0020
8	-243024.5	-40.9	31.8	0.0574
9	-243030.9	-47.3	19.0	0.0011
10	-243017.6	-33.9	20.8	0.0090
11	-243052.1	-68.4	30.3	0.0010
12	-243070.6	-86.9	37.3	0.0013
13	-243066.1	-82.5	40.4	0.0122
14	-243143.1	-159.4	39.6	0.0000
15	-243151.3	-167.7	43.3	0.0000
16	-243186.7	-203.0	42.2	0.0000

Table 4: (Continued)

17	-243102.9	-119.3	36.6	0.0001
18	-243167.6	-184.0	37.8	0.0000
19	-243155.4	-171.7	38.9	0.0000
20	-243065.3	-81.7	29.6	0.0007
21	-243017.6	-33.9	20.8	0.0121
22	-243030.9	-47.3	19.0	0.0006
23	-243068.3	-84.7	29.9	0.0009
24	-243103.9	-120.3	36.7	0.0000
25	-243135.2	-151.5	39.0	0.0000

Table 5:

(C)
Mycobacterium tuberculosis

#	Likelihood	ΔL	$\sigma \Delta L$	RELL-BP
1	-242983.7	best	N/A	0.8589
2	-243160.7	-177.0	46.5	0.0000
3	-243192.5	-208.9	48.9	0.0000
4	-243216.2	-232.5	48.6	0.0000
5	-243140.3	-156.6	44.1	0.0000
6	-243146.6	-163.0	48.1	0.0000
7	-243153.9	-170.3	48.0	0.0000
8	-243071.4	-87.7	41.0	0.0013
9	-243023.4	-39.7	34.2	0.0443
10	-243037.2	-53.5	33.3	0.0052
11	-243098.4	-114.7	39.6	0.0000
12	-243126.1	-142.4	44.5	0.0000
13	-243146.5	-162.8	46.9	0.0000
14	-243087.0	-103.3	52.5	0.0010
15	-243128.5	-144.8	54.7	0.0000
16	-243150.8	-167.2	54.1	0.0000
17	-243079.5	-95.9	49.1	0.0014
18	-243136.6	-153.0	50.5	0.0000
19	-243152.6	-168.9	49.7	0.0000
20	-243062.9	-79.3	41.5	0.0012
21	-243037.2	-53.5	33.3	0.0059
22	-243023.4	-39.7	34.2	0.0327
23	-243047.8	-64.1	43.2	0.0209
24	-243062.5	-78.8	49.7	0.0192
25	-243076.6	-93.0	51.9	0.0080

two types of information appear to differ substantially. The gene presence-absence analysis seemed to be dominated by the phenotypic signal, primarily that from gene loss. The tree based on conserved gene pairs appeared to combine phylogenetic information with major effects of horizontal transfer of operons. In contrast, the trees based on the distributions of the identity level of orthologs appear to be more meaningful phylogenetically

as indicated by the recovery of established high-level phylogenetic groups of bacteria, such as Proteobacteria and Gram-positive bacteria. The ability to correctly identify these major bacterial subdivisions and the absence of obviously wrong groupings confer credibility to non-trivial clades present in these trees, in particular the spirochete-chlamydia clade. The same logic applied to the tree made of concatenated ribosomal protein sequences,

Table 6:(D)
Synechocystis sp.

#	Likelihood	ΔL	$\sigma\Delta L$	RELL-BP
1	-242983.7	best	N/A	0.9617
2	-243118.5	-134.8	47.5	0.0000
3	-243077.9	-94.3	51.4	0.0265
4	-243115.8	-132.1	50.9	0.0000
5	-243084.6	-101.0	46.4	0.0031
6	-243184.5	-200.8	46.3	0.0000
7	-243208.1	-224.4	45.5	0.0000
8	-243135.7	-152.1	38.1	0.0000
9	-243072.3	-88.6	32.1	0.0006
10	-243083.7	-100.0	31.6	0.0000
11	-243099.4	-115.7	40.6	0.0000
12	-243102.5	-118.8	45.2	0.0003
13	-243097.2	-113.5	47.6	0.0030
14	-243204.5	-220.8	48.0	0.0000
15	-243279.8	-296.2	49.3	0.0000
16	-243288.4	-304.7	49.4	0.0000
17	-243194.3	-210.7	42.9	0.0000
18	-243180.8	-197.1	49.5	0.0000
19	-243177.5	-193.8	49.4	0.0000
20	-243090.1	-106.4	41.4	0.0038
21	-243083.7	-100.0	31.6	0.0000
22	-243072.3	-88.6	32.1	0.0010
23	-243129.2	-145.5	38.5	0.0000
24	-243165.6	-181.9	45.1	0.0000
25	-243195.5	-211.9	47.6	0.0000

Table 7:(E)
The Demococcus-Mycobacterium-Synechocystis clade

#	Likelihood	ΔL	$\sigma\Delta L$	RELL-BP
1	-242983.7	0.0	<-best	0.7280
2	-243065.3	-81.7	34.7	0.0000
3	-243122.4	-138.8	37.2	0.0000
4	-243148.7	-165.1	35.8	0.0000
5	-243053.8	-70.1	28.9	0.0001
6	-243103.1	-119.5	33.6	0.0000
7	-243096.4	-112.7	34.1	0.0001
8	-243003.1	-19.4	23.2	0.1697
9	-243010.5	-26.9	21.5	0.0560
10	-243028.9	-45.3	31.2	0.0419
11	-243054.3	-70.7	34.7	0.0042

Table 8:(F)
The spirochaete-chlamydia clade

#	Likelihood	ΔL	$\sigma\Delta L$	RELL-BP
1	-242983.7	best	N/A	0.6173
2	-243055.2	-71.5	21.5	0.0000
3	-243050.7	-67.1	34.7	0.0078
4	-243096.8	-113.2	33.0	0.0000
5	-243045.5	-61.9	25.0	0.0007
6	-243066.5	-82.8	32.8	0.0012
7	-243072.2	-88.5	32.4	0.0006
8	-243049.0	-65.3	25.2	0.0005
9	-243036.7	-53.1	21.7	0.0016
10	-243057.4	-73.7	21.9	0.0000
11	-242998.3	-14.6	40.2	0.3605
12	-243086.4	-102.7	36.2	0.0000
13	-243024.8	-41.1	28.0	0.0071
14	-243146.2	-162.5	31.4	0.0000
15	-243130.7	-147.0	32.9	0.0000
16	-243077.2	-93.6	23.4	0.0000
17	-243036.9	-53.3	22.1	0.0027

Table 9:(G)
 ϵ -proteobacteria

#	Likelihood	ΔL	$\sigma\Delta L$	RELL-BP
1	-242983.7	best	N/A	0.5482
2	-243093.9	-110.3	32.7	0.0000
3	-243009.8	-26.1	39.6	0.0417
4	-242991.7	-8.0	41.2	0.3788
5	-243007.7	-24.0	34.1	0.0308
6	-243121.1	-137.4	30.3	0.0000
7	-243112.4	-128.7	31.1	0.0000
8	-243076.4	-92.8	22.0	0.0000
9	-243071.1	-87.4	29.7	0.0000
10	-243055.0	-71.4	33.4	0.0005

which included two other non-trivial bacterial groupings, *Aquifex-Thermotoga* and *Synechocystis-Mycobacterium-Deinococcus*, the latter joining the Gram-positive branch. Furthermore, extensive testing of alternative topologies using the Kishino-Hasegawa test largely supported these new bacterial branches. The nature of this support becomes clearer when one examines the re-

sults of the protein family census. Each of the potential new clades was indeed most common among the observed topologies, but in no case, was the excess of this topology overwhelming. Taken together, these results seem to shed light on the very notion of a "species tree". It appears that, at best, a species tree can be viewed as a

Table 10:(H)
Crenarchaeota and Euryarchaeota

#	Likelihood	ΔL	$\sigma \Delta L$	RELL-BP
1	-242983.7	best	N/A	0.5840
2	-242993.2	-9.5	33.7	0.4160

^aThe numbers correspond to those in Fig. 5 ^bThe likelihood difference with the first (original) topology ^cThe standard deviation of the above ^dThe bootstrap probability of the given topology estimated with REll method [49].

Table 11: COGs used for the comparative analysis of Maximum Likelihood trees for individual protein families

COG	spec ^a	prot ^b	Name
COG0012	40	41	Predicted GTPase
COG0013	40	40	Alanyl-tRNA synthetase
COG0016	40	40	Phenylalanyl-tRNA synthetase alpha submit
COG0018	40	41	Arginyl-tRNA synthetase
COG0020	37	40	Undecaprenyl pyrophosphate synthase
COG0048	39	39	Ribosomal protein S12
COG0049	40	41	Ribosomal protein S7
COG0051	40	40	Ribosomal protein S10
COG0052	40	40	Ribosomal protein S2
COG0060	40	40	Isoleucyl-tRNA synthetase
COG0061	37	40	Predicted kinase
COG0064	30	30	Asp-tRNAAsn/Glu-tRNAIn amidotransferase B subunit (PET 112 homolog)
COG0072	40	40	Phenylalanyl-tRNA synthetase beta subunit
COG0080	40	41	Ribosomal protein L1 I
COG0081	40	40	Ribosomal protein L1
COG0082	33	33	Chorismate synthase
COG0085	40	40	DNA-directed RNA polymerase beta subunit/140 kD subunit (split gene in Mjan, Mthe, Aful)
COG0087	40	40	Ribosomal protein L3
COG0088	40	40	Ribosomal protein L4
COG0090	40	40	Ribosomal protein L2
COG0091	40	40	Ribosomal protein L22
COG0092	40	40	Ribosomal protein S3
COG0093	39	39	Ribosomal protein L1 4
COG0094	40	40	Ribosomal protein L5
COG0096	40	40	Ribosomal protein S8
COG0097	40	40	Ribosomal protein L6
COG0098	40	40	Ribosomal protein S5
COG0099	40	40	Ribosomal protein S13
COG0100	39	39	Ribosomal protein S11
COG0101	38	38	Pseudouridylate synthase (tRNA psi55)
COG0102	40	40	Ribosomal protein L1 3
COG0103	40	40	Ribosomal protein S9
COG0104	31	31	Adenylosuccinate synthase
COG0105	33	33	Nucleoside diphosphate kinase
COG0126	39	39	3-phosphoglycerate kinase
COG0127	34	35	Xanthosine triphosphate pyrophosphatase
COG0128	33	35	5-enolpyruvylshikimate-3-phosphate synthase
COG0130	37	37	Pseudouridine synthase
COG0134	30	30	Indole-3-glycerol phosphate synthase
COG0135	30	30	Phosphoribosylanthranilate isomerase

Table II: COGs used for the comparative analysis of Maximum Likelihood trees for individual protein families (Continued)

COG0143	40	41	Methionyl-tRNA synthetase
COG0148	39	43	Enolase
COG0149	39	41	Triosephosphate isomerase
COG0151	30	30	Phosphoribosylamine-glycine ligase
COG0152	30	32	Phosphoribosylaminoimidazolesuccinocarboxamide (SAICAR) synthase
COG0159	31	31	Tryptophan synthase alpha chain
COG0162	40	43	Tyrosyl-tRNA synthetase
COG0164	35	35	Ribonuclease HII
COG0166	35	35	Glucose-6-phosphate isomerase
COG0167	32	37	Dihydroorotate dehydrogenase
COG0169	33	39	Shikimate 5-dehydrogenase
COG0171	35	37	NAD synthase
COG0172	40	40	Seryl-tRNA synthetase
COG0173	30	30	Aspartyl-tRNA synthetase
COG0178	31	33	Excinuclease ATPase submit
COG0180	40	43	Tryptophanyl-tRNA synthetase
COG0190	33	33	5,10-methylene-tetrahydrofolate dehydrogenase
COG0193	30	30	Peptidyl-tRNA hydrolase
COG0197	40	40	Ribosomal protein L16/L10E
COG0198	40	40	Ribosomal protein L24
COG0200	40	40	Ribosomal protein L1 5
COG0201	40	41	Preprotein translocase subunit SecY
COG0202	40	40	DNA-directed RNA polymerase alpha subunit/40 kD subunit
COG0203	30	30	Ribosomal protein L1 7
COG0215	38	39	Cysteinyl-tRNA synthetase
COG0216	30	30	Protein chain release factor A
COG0221	31	31	Inorganic pyrophosphatase
COG0222	30	30	Ribosomal protein L7/L12
COG0223	30	34	Methionyl-tRNA formyltransferase
COG0231	40	46	Translation elongation factor P/translation initiation factor eIF-5A
COG0233	30	30	Ribosome recycling factor
COG0237	39	41	Dephospho-CoA kinase
COG0242	30	35	N-formylmethionyl-tRNA deformylase
COG0244	40	40	Ribosomal protein L10
COG0250	40	43	Transcription antiterminator
COG0256	40	40	Ribosomal protein L1 8
COG0258	40	47	5'-3' exonuclease (including N-terminal domain of PolI)
COG0261	30	30	Ribosomal protein L21
COG0264	30	30	Translation elongation factor Ts
COG0272	30	31	NAD-dependent DNA ligase (contains BRCT domain type II)
COG0275	30	30	Predicted S-adenosylmethionine-dependent methyltransferase involved in cel envelope biogenesisI
COG0284	32	32	Orotidine-5'-phosphate decarboxylase
COG0290	30	30	Translation initiation factor IF3
COG0292	30	30	Ribosomal protein L20
COG0294	33	36	Dihydropteroate synthase
COG0305	30	31	Replicative DNA helicase
COG0313	30	31	Predicted methyltransferases
COG0319	30	30	Predicted metal-dependent hydrolase
COG0335	30	30	Ribosomal protein L1 9
COG0336	30	30	tRNA-(guanine-N1)-methyltransferase
COG0340	32	34	Biotin-(acetyl-CoA carboxylase) ligase
COG0343	35	36	Queuine/archaeosine tRNA-ribosyltransferase
COG0351	31	34	Hydroxymethylpyrimidine/phosphomethylpyrimidine kinase
COG0359	30	30	Ribosomal protein L9
COG0441	40	43	Threonyl-tRNA synthetase
COG0442	40	40	Prolyl-tRNA synthetase
COG0452	32	32	Phosphopantothenoilcysteine synthetase/decarboxylase
COG0461	33	34	Orotate phosphoribosyltransferase
COG0462	37	40	Phosphoribosylpyrophosphate synthetase
COG0481	30	30	Membrane GTPase LepA
COG0495	40	41	Leucyl-tRNA synthetase
COG0504	38	38	CTP synthase (UTPammonia lyase)

Table 11: COGs used for the comparative analysis of Maximum Likelihood trees for individual protein families (Continued)

COG0519	33	33	GMP synthase – PP-ATPase domain
COG0522	40	40	Ribosomal protein S4 and related proteins
COG0525	40	40	Valyl-tRNA synthetase
COG0528	40	40	Uridylate kinase
COG0532	40	40	Translation initiation factor 2 (GTPase)
COG0533	40	40	Metal-dependent proteases with possible chaperone activity
COG0536	30	30	Predicted GTPase
COG0540	30	30	Aspartate carbamoyltransferase, catalytic chain
COG0541	40	40	Signal recognition particle GTPase
COG0544	30	30	FKBP-type peptidyl-prolyl cis-trans isomerase (trigger factor)
COG0547	30	35	Anthranilate phosphoribosyltransferase
COG0552	40	40	Signal recognition particle GTPase
COG0556	31	31	Helicase subunit of the DNA excision repair complex
COG0571	30	30	dsRNA-specific ribonuclease
COG0573	30	34	ABC-type phosphate transport system, permease component
COG0576	34	35	Molecular chaperone GrpE (heat shock protein)
COG0581	30	34	ABC-type phosphate transport system, permease component
COG0587	30	35	DNA polymerase III alpha subunit
COG0597	30	30	Lipoprotein signal peptidase
COG0653	30	32	Preprotein translocase subunit SecA (ATPase, RNA helicase)
COG0682	30	30	Prolipoprotein diacylglyceryltransferase
COG0691	30	30	tmRNA-binding protein
COG0706	30	34	Preprotein translocase subunit YidC
COG0781	30	30	Transcription termination factor
COG0858	30	30	Ribosome-binding factor A
COG1160	30	30	Predicted GTPases
COG1214	30	30	Inactive homologs of metal-dependent proteases, putative molecular chaperones
COG1466	30	30	DNA polymerase III delta subunit
COG1488	32	35	Nicotinic acid phosphoribosyltransferase
COG2812	30	30	DNA polymerase III, gamma/tau subunits

^aNumber of represented species. ^bNumber of proteins.

prevailing phylogenetic trend, which, as far as deep branchings are concerned, may not even apply to a majority of the genes in a genome.

The potential new, deep relationships between bacterial lineages revealed during this analysis should be considered preliminary and treated with caution. Nevertheless, an evolutionary affinity between Cyanobacteria (*Synechocystis*) and Actinomycetes (*Mycobacterium*) appears plausible, particularly given the presence, in these bacterial groups, of well-developed and partly similar signal transduction systems [27]. The connection between two hyperthermophilic bacteria, *Aquifex* and *Thermotoga*, also has obvious biological meaning, although, in this case, particular caution is due, given the possibility of preferential horizontal gene exchange between these organisms that inhabit similar environments. However, the strong support for this grouping obtained in the analysis of concatenated ribosomal proteins argues against horizontal transfer as the primary cause for the observed topology. Although recent studies on the phylogeny of ribosomal proteins suggest some horizontal transfer events, these seem to be largely restricted to bacteria-

specific ribosomal proteins. In the universal set of ribosomal proteins, only one, S14, showed clear signs of horizontal transfer [28]. The potential deep phylogenetic connections uncovered during this analysis call for detailed genome comparisons in search of potential shared derived characters, such as unique protein domain architectures, that could support the new clades.

The major bacterial lineages are poorly resolved in rRNA-based trees [2,29] and those built using alignments of RNA polymerase subunits [30] and translation elongation factors [29,31]. In the currently accepted taxonomy, which is based primarily (but not exclusively) on 16S RNA phylogenetic analysis, bacterial lineages that are suggested by this analysis to form higher-level clusters, tend to form primary nodes under Bacteria (Chlamydiales, Spirochetales, Cyanobacteria, the *Thermus-Deinococcus* group, Aquificales, Thermotogales). Thus, the genome trees primarily suggest (however tentatively) new unifications based on deep phylogenetic connections, rather than split already established clades. A notable exception is the traditional unification of Actinomycetes, or High G+C gram-positive bacteria (repre-

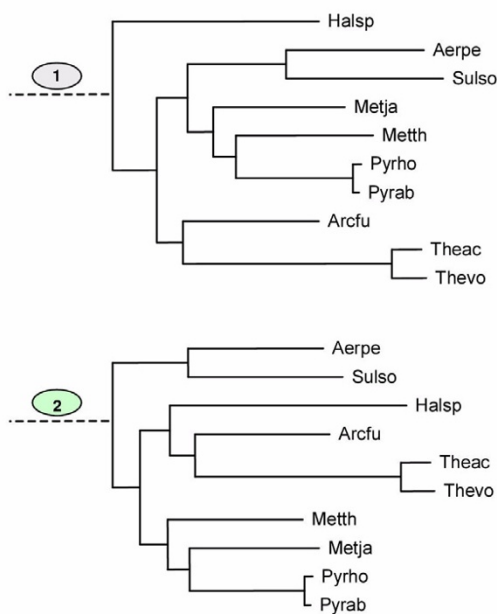


Figure 12
The Kishino-Hasegawa test for position of Crenarchaeota with respect to Euryarchaeota. Position of Crenarchaeota with respect to Euryarchaeota (1) – the maximum-likelihood tree topology; (2) – the competing topology with Crenarchaeota and Euryarchaeota as sister groups. See Table 10

sented here by *Mycobacterium*), with low G+C Gram-positive bacteria (the *Bacillus-Clostridium* group) under Firmicutes (Gram-positive bacteria). Such a connection was not supported by any of the trees analyzed here, and it is also poorly, if at all, supported by the latest consensus trees for 16S RNA, 23 S RNA and translation factor EF-Tu [29]. Therefore it seems likely that the Firmicutes clade, at least in its present composition, does not exist. The new clade that might replace it consists of low-GC Gram-positive bacteria and the potential Actinomycetes-Deinococcales-Cyanobacteria group (Fig. 6). All methods of tree analysis applied here also challenge the traditional division of the archaeal kingdom into Euryarchaeota and Crenarchaeota, suggesting instead that Euryarchaeota could be a paraphyletic group with respect to Crenarchaeota, or in other words, that Crenarchaeota might have evolved from within the Euryarchaeota. However, the existence of a statistically supported alternative topology, with a sister-group relationship between Euryarchaeota and Crenarchaeota allows for the possibility that the apparent paraphyly of Euryarchaea is

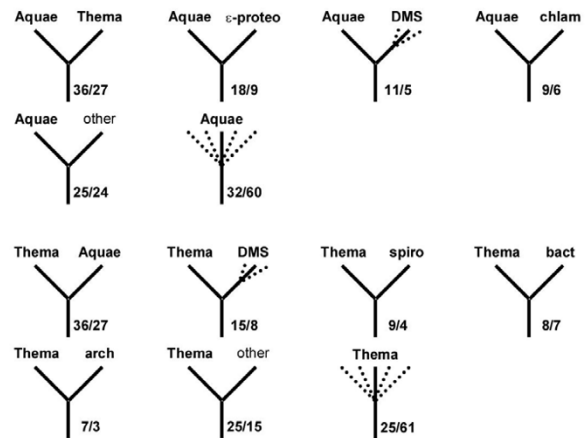


Figure 13
A census of the topologies of maximum-likelihood trees for individual protein families. *Thermotoga* and *Aquifex*. In each panel, the left top icon shows the grouping tested and the remaining icons show the most common alternative topologies for the given species/group. Dotted lines indicate optional presence of (possibly several) members of the indicated group (e.g. "proteo" with several dotted lines leading to it means that any number and combination of proteobacterial proteins could be present on the given branch). For each icon, the number of COG trees with the given topology (upper number) and the size of the subset supported by at least 70% bootstrap values (lower number) are indicated. Uncertain topologies (lacking clearly defined taxonomic units on the other side of the subtree or those without bootstrap support) are indicated by multiple dotted lines without indication of the neighbor. Abbreviations: TA – Thema and/or Aquae; DMS – any combination of Deira, Myctu and SynPC. Note that, in some cases, which involve taxonomic clades rather than single organisms (e.g. spirochetes), failure of the corresponding species to form a clade in the given tree may lead to asymmetrical counts of topologies. For example, if a particular tree has a (Deira,(Trep, Borbu)) branch, this tree will be included in both the Deira-spiro and spiro-Deira tallies. If, however, the subtree ((Deira, Trep),(Aquae, Borbu)) is present, then the Deira-spiro and Aquae-spiro tallies gain one count each, but the spiro-Deira and spiro-Aquae tallies do not; instead, a case of spirochete polyphyly is registered.

an artifact caused by rapid evolution in some Euryarchaeal lineages, such as *Halobacterium* and *Thermoplasma*.

An independent phylogenetic study of concatenated ribosomal proteins has been recently published [32]. The main specific conclusion reported in this study was the apparent association of *Synechocystis* with Gram-positive bacteria, although instability of the tree topology de-

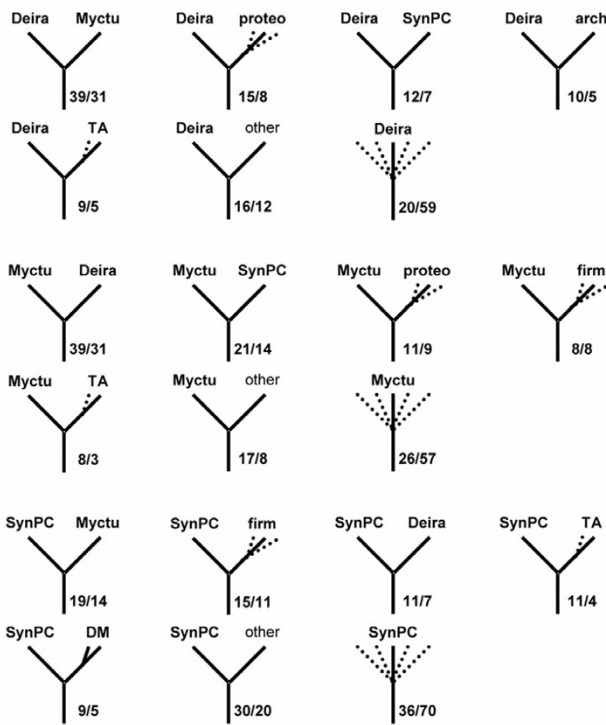


Figure 14
A census of the topologies of maximum-likelihood trees for individual protein families. *Deinococcus*, *Mycobacterium* and *Synechocystis*. The designations are as in Fig. 3.

pendent on the subset of sites used for analysis was noticed. Another recent study addressed the issue of a global tree through phylogenetic analysis of 14 concatenated sets of orthologous proteins, for which no strong evidence of horizontal transfer was available [33]. Notably, some of the unexpected groupings within the bacterial domain reported in this study coincide or overlap with those described here, namely, a spirochete-chlamydial clade and a Deinococcales-Cyanobacteria clade. The grouping of the latter clade with Actinomycetes, the unification of the Deinococcales-Cyanobacteria-Actinomycetes clade with Gram-positive bacteria and the grouping of the two bacterial hyperthermophiles were not reproduced in the work of Brown and co-workers. The differences between the results of the two studies could owe to the differences between data sets analyzed, the methods used or, most likely, both. We should note that the present study engaged a substantially broader data set and more diverse methods for tree construction. We believe, however, that, in terms of the potential contribution of genome-wide phylogenetic analysis to phylogenetic taxonomy, the areas where different methods and independent analyses by different groups converge might be more important than the areas of discrepancy. It appears that potential new clades re-

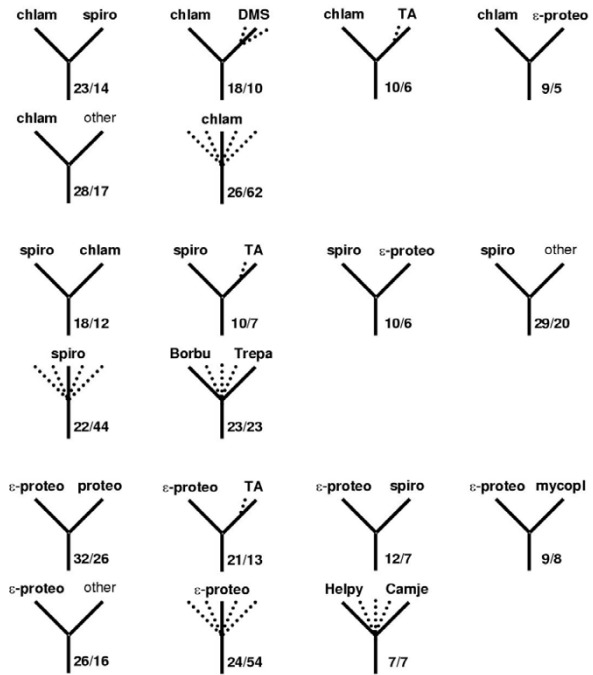


Figure 15
A census of the topologies of maximum-likelihood trees for individual protein families. Spirochetes, chlamydia and epsilon-proteobacteria. The designations are as in Fig. 3.

vealed in such independent studies are strong candidates for new, high-level taxa.

The results of the present study suggest that genome trees based on new, integral criteria do not provide substantial advantages in phylogenetic reconstruction over more traditional, alignment-based methods expanded to the genomic scale. In fact, the latter seem to be more sensitive in detecting potential deep evolutionary relationships and this is expected to further improve with the increasing number of completely sequenced genomes becoming available for analysis. We believe, however, that this conclusion does not necessarily indicate that genome trees, such as those based on representation of genomes in orthologous sets or conservation of gene pairs, are useless. In addition to revealing some new phylogenetic affinities, they are capable of alerting researchers to other evolutionary phenomena, such as loss of similar gene sets in different organisms and preferential horizontal gene exchange between certain lineages.

Material and Methods

Sequence data

The sequences of the proteins encoded in complete genomes were extracted from the Genome division of the

Entrez retrieval system [34]. The analyzed genomes included those of 30 bacteria: *Aquifex aeolicus* (Aqua), *Bacillus halodurans* (Bacha), *Bacillus subtilis* (Bacsu), *Borrelia burgdorferi* (Borbu), *Buchnera sp.* (Bucsp), *Campylobacter jejunii* (Camje), *Caulobacter crescentus* (Caucr), *Chlamydia trachomatis* (Chltr), *Chlamydomo-phi-la pneumoniae* (Chlpn), *Deinococcus radiodurans* (Deira), *Escherichia coli* (Escco), *Haemophilus influenzae* (Haein), *Helicobacter pylori* (Helpy), *Lactococcus lactis* (Lacla), *Mesorhizobium loti* (Meslo), *Mycoplasma genitalium* (Mycge), *Mycoplasma pneumoniae* (Mycpn), *Mycobacterium tuberculosis* (Myctu), *Neisseria meningitidis* (Neime), *Pasteurella multocida* (Pasmu), *Pseudomonas aeruginosa* (Pseae), *Rickettsia prowazekii* (Ricpr), *Staphylococcus aureus* (Staa), *Streptococcus pyogenes* (Strpy), *Synechocystis PCC6803* (SynPC), *Thermotoga maritima* (Thema), *Treponema pallidum* (Trep), *Ureaplasma urealyticum* (Ureur), *Vibrio cholerae* (Vibch), *Xylella fastidiosa* (Xylfa), and ten archaea: *Aeropyrum pernix* (Aerpe), *Archaeoglobus fulgidus* (Arcfu), *Halobacterium sp.* (Halsp), *Methanobacterium thermoautotrophicum* (Metth), *Methanococcus jannaschii* (Metja), *Pyrococcus horikoshii* (Pyrho), *Pyrococcus abyssi* (Pyrab), *Sulfolobus solfataricus* (Sulso), *Thermoplasma acidophilum* (Theac), *Thermoplasma volcanium* (Thevo).

Phylogenetic tree construction

Parsimony trees based on the presence-absence of conserved gene pairs in prokaryotic genomes

The database of Clusters of Orthologous Groups of proteins (COGs) was used as the source of information on orthologous genes in prokaryotic genomes [35,36]. Briefly, the COGs were constructed from the results of all-against-all BLAST [37] comparison of proteins encoded in complete genomes by detecting consistent groups of genome-specific best hits (BeTs). The COG construction procedure does not rely on any preconceived phylogenetic tree of the included species except that certain obviously related genomes (for example, two species of mycoplasmas or pyrococci) were grouped prior to the analysis, to eliminate strong dependence between BeTs. In order to avoid spurious occurrence of the same gene pair, only gene pairs conserved in three or more genomes were considered. A pair of genes from two COGs was considered to be conserved if the respective genes were adjacent in at least one genome and were separated by no more than two genes in at least two additional genomes. This relaxed definition of a conserved gene pair was adopted to take into account the high level of recombination in prokaryotic genomes. From the data on the presence-absence of each conserved gene pair in the analyzed genomes (excluding pairs of closely related species: *E. coli*-*Buchnera sp.*, *H. influenzae*-*P. multocida*, *C. trachomatis*-*C. pneumoniae*, *P. horikoshii*-*P. ab-*

yssi, *M. genitalium*-*M. pneumoniae*-*U. urealyticum*, *H. pyroli* – *C. jejuni*, *T. acidophilum*-*T. volcanium*), a 0/1 matrix analogous to the one used for the presence-absence of individual genes was constructed, and a tree was built using Dollo parsimony [38]. A parsimony method was chosen for this analysis because the presence-absence of a conserved gene pair in a genome can be naturally treated in terms of character states. The Dollo model is based on the assumption that each derived character state (in this case, the presence of a gene pair) originates only once, and homoplasies exist only in the form of reversals to the ancestral condition (absence of a gene pair) [38]. In other words, parallel or convergent gains of the derived condition are assumed to be highly unlikely. The Dollo parsimony method is not sensitive to gene loss which is extremely common in evolution of prokaryotes, but the results can be affected by independent acquisition of the same gene pair by different genome via horizontal gene transfer. Phylogenetic analysis was performed by using the PAUP 4.0 program [39], with 1000 bootstrap replicates performed to assess the reliability of the tree topology. In addition, the tree topology was analyzed using the neighbor-joining method [40].

Parsimony trees based on the representation of genomes in orthologous gene sets

The information on orthologous genes in prokaryotic genomes and the yeast genome was derived from the COGs as in the previous approach, and the orthology data were similarly represented as a 0/1 matrix of presence-absence of the analyzed genomes in the COGs. A Dollo parsimony tree was constructed and the reliability of its topology was assessed using the bootstrap method as described above.

Distance trees based on distributions of identity percentage between orthologous protein sequences

The sequences of all proteins encoded in the analyzed genomes were compared to each other using the gapped BLASTP program [37]. Reciprocal, genome-specific BeTs were collected at different expectation (E) value cutoffs (0.01, 0.001, 0.0001, 0.00001). This method for identification of probable orthologs is, in principle, similar to the method employed in COG construction, but differs in that there is no requirement for the formation of triangles of consistent BeTs. The result of this procedure is a conservative selection of orthologous pairs because the cases of lineage-specific duplication that result in non-symmetrical BeTs are excluded and so are orthologous pairs with very low sequence similarity. However, the limitation of the COG system, namely the requirement that each orthologous group is represented in at least three genomes, is avoided. The distributions of identity percentage among the reciprocal best hits were derived for each pair of species. The mean, mode, medi-

an and different quantiles of the identity percentage distributions were used for estimating evolutionary distances. Four distance measures were used, namely: i) P-distances calculated as the fraction of different residues: $d = 1 - q$, ii) Poisson distances $d = -\ln u$, iii) geometric distances calculated using the formula $d = 1/u - 1$, and iv) logarithmic distances found as a solution of the equation $u = \ln(1 + 2d)/(2d)$, where d is the evolutionary distance, q is percent identity, and $u = (q - 0.05)/0.95$ [41,42][43]. Trees were constructed from the distance matrices obtained with the above distance estimates using the neighbor-joining method [40] as implemented in the NEIGHBOR program of the PHYLIP package [44]. Bootstrap values were estimated by resampling the set of orthologs identified for each pair of genomes 1000 times and reconstructing trees from the distributions of the distances from these resampled sets.

Maximum Likelihood trees based on concatenated alignments of ribosomal proteins

Sets of orthologous ribosomal proteins were extracted from the COG database, and their amino acid sequences were aligned using the T-Coffee program [45], with subsequent manual validation and removal of poorly aligned regions. The alignments are available upon request. Pairwise evolutionary distances between the sequences in concatenated alignments were calculated using the Dayhoff PAM model as implemented in the PROTDIST program of the PHYLIP package [44]. A distance tree was constructed from the resulting distance matrix by using the least-square [46] method as implemented in the FITCH program of PHYLIP [44]. The maximum likelihood tree was constructed with the JTT-F model of amino acid substitutions [47], as implemented in the ProtML program of the MOLPHY package [48], by optimizing the least squares tree with local rearrangements. Alternative topologies were created manually by modifications of the original tree and directly compared by ProtML. Bootstrap analysis was performed by using the Resampling of Estimated Log-Likelihoods (RELL) method as implemented in ProtML [48,49].

Comparative analysis of Maximum Likelihood trees for individual protein families

The representative families were selected from the COG database according to the following criteria: i) at least 30 species are represented; ii) no more than two paralogs in any of the species; iii) no more than 1.2 paralogs per genome on average; iv) at least 100 positions in the alignment containing less than 30% of gaps. This selection procedure resulted in a set of 132 families (COGs). Alignments and ML trees were constructed for these families as described above for the concatenated ribosomal proteins.

Quantitative comparison of tree topologies

To compare tree topologies quantitatively, the symmetric distance between trees [50] was computed using the TREEDIST program of the PHYLIP package (version 3.6a). Briefly, each of the two compared trees is divided by each internal branch into two partitions. The symmetric distance is the number of partitions that are found in one tree but not the other.

Acknowledgements

We thank M. Nei for stimulating discussions about the Dollo parsimony analysis, J. Felsenstein for alerting us of the inclusion of the TREEDIST program in PHYLIP3.6a and D. Leipe for discussions on taxonomy.

References

1. Woese CR: **Bacterial evolution.** *Microbiol Rev* 1987, **51**:221-271
2. Olsen GJ, Woese CR, Overbeek R: **The winds of (evolutionary) change: breathing new life into microbiology.** *J Bacteriol* 1994, **176**:1-6
3. Doolittle RF, Feng DF, Tsang S, Cho G, Little E: **Determining divergence times of the major kingdoms of living organisms with a protein clock.** *Science* 1996, **271**:470-477
4. Teichmann SA, Mitchison G: **Is there a phylogenetic signal in prokaryote proteins?** *J Mol Evol* 1999, **49**:98-107
5. Sicheritz-Ponten T, Andersson SG: **A phylogenomic approach to microbial evolution.** *Nucleic Acids Res* 2001, **29**:545-552
6. Doolittle WF: **Phylogenetic classification and the universal tree.** *Science* 1999, **284**:2124-2129
7. Doolittle WF: **Lateral genomics.** *Trends Cell Biol* 1999, **9**:M5-8
8. Snel B, Bork P, Huynen MA: **Genome phylogeny based on gene content.** *Nat Genet* 1999, **21**:108-110
9. Fitz-Gibbon ST, House CH: **Whole genome-based phylogenetic analysis of free-living microorganisms.** *Nucleic Acids Res* 1999, **27**:4218-4222
10. Tekala F, Dujon B: **Pervasiveness of gene conservation and persistence of duplicates in cellular genomes.** *J Mol Evol* 1999, **49**:591-600
11. Grishin NV, Wolf YI, Koonin EV: **From complete genomes to measures of substitution rate variability within and between proteins.** *Genome Res* 2000, **10**:991-1000
12. Dobzhansky T, Sturtevant AH: **Inversions in the chromosomes of *Drosophila pseudoobscura*.** *Genetics* 1938, **23**:28-64
13. Hannehalli S, Chappay C, Koonin EV, Pevzner PA: **Genome sequence comparison and scenarios for gene rearrangements: a test case.** *Genomics* 1995, **30**:299-311
14. Sankoff D, Blanchette M: **Phylogenetic invariants for genome rearrangements.** *J Comput Biol* 1999, **6**:431-445
15. Mushegian AR, Koonin EV: **Gene order is not conserved in bacterial evolution.** *Trends Genet* 1996, **12**:289-290
16. Dandekar T, Snel B, Huynen M, Bork P: **Conservation of gene order: a fingerprint of proteins that physically interact.** *Trends Biochem Sci* 1998, **23**:324-328
17. Huynen MJ, Snel B: **Gene and context: integrative approaches to genome analysis.** *Adv. Prot. Chem* 2000, **54**:345-379
18. Tatusov RL, Mushegian AR, Bork P, Brown NP, Hayes WS, Borodovsky M, Rudd KE, Koonin EV: **Metabolism and evolution of *Haemophilus influenzae* deduced from a whole-genome comparison with *Escherichia coli*.** *Curr Biol* 1996, **6**:279-291
19. Overbeek R, Fonstein M, D'Souza M, Pusch GD, Maltsev N: **The use of gene clusters to infer functional coupling.** *Proc Natl Acad Sci USA* 1999, **96**:2896-2901
20. Fujibuchi W, Ogata H, Matsuda H, Kanehisa M: **Automatic detection of conserved gene clusters in multiple genomes by graph comparison and P-quasi grouping.** *Nucleic Acids Res* 2000, **28**:4029-4036
21. Wolf YI, Rogozin IB, Kondrashov AS, Koonin EV: **Genome alignment, evolution of prokaryotic genome organization and prediction of gene function using genomic context.** *Genome Res* 2001
22. Koonin EV, Mushegian AR, Galperin MY, Walker DR: **Comparison of archaeal and bacterial genomes: computer analysis of pro-**

- tein sequences predicts novel functions and suggests a chimeric origin for the archaea. *Mol Microbiol* 1997, **25**:619-637
23. Aravind L, Tatusov RL, Wolf YI, Walker DR, Koonin EV: **Evidence for massive gene exchange between archaeal and bacterial hyperthermophiles.** *Trends Genet* 1998, **14**:442-444
 24. Nelson KE, Clayton RA, Gill SR, Gwinn ML, Dodson RJ, Haft DH, Hickey EK, Peterson JD, Nelson WC, Ketchum KA, McDonald L, Utterback TR, Malek JA, Linher KD, Garrett MM, Stewart AM, Cotton MD, Pratt MS, Phillips CA, Richardson D, Heidelberg J, Sutton GG, Fleischmann RD, Eisen JA, Fraser CM, et al: **Evidence for lateral gene transfer between Archaea and bacteria from genome sequence of *Thermotoga maritima*.** *Nature* 1999, **399**:323-329
 25. Martin W: **Mosaic bacterial chromosomes: a challenge en route to a tree of genomes.** *Bioessays* 1999, **21**:99-104
 26. Pace NR: **A molecular view of microbial diversity and the biosphere.** *Science* 1997, **276**:734-740
 27. Ponting CP, Aravind L, Schultz J, Bork P, Koonin EV: **Eukaryotic signalling domain homologues in archaea and bacteria. Ancient ancestry and horizontal gene transfer.** *J Mol Biol* 1999, **289**:729-745
 28. Brochier C, Philippe H, Moreira D: **The evolutionary history of ribosomal protein RpS14: horizontal gene transfer at the heart of the ribosome.** *Trends Genet* 2000, **16**:529-533
 29. Ludwig W, Strunk O, Klugbauer S, Klugbauer N, Weizenegger M, Neumaier J, Bachleitner M, Schleifer KH: **Bacterial phylogeny based on comparative sequence analysis.** *Electrophoresis* 1998, **19**:554-568
 30. Gruber TM, Bryant DA: **Molecular systematic studies of eubacteria, using sigma70-type sigma factors of group I and group J Bacterial** 1997, **179**:1734-1747
 31. Baldauf SL, Palmer JD, Doolittle WF: **The root of the universal tree and the origin of eukaryotes based on elongation factor phylogeny.** *Proc Natl Acad Sci USA* 1996, **93**:7749-7754
 32. Hansmann S, Martin W: **Phylogeny of 33 ribosomal and six other proteins encoded in an ancient gene cluster that is conserved across prokaryotic genomes: influence of excluding poorly alignable sites from analysis.** *Int J Syst Evol Microbiol* 2000, **50 Pt 4**:1655-1663
 33. Brown JR, Douady CJ, Italia MJ, Marshall WE, Stanhope MJ: **Universal trees based on large combined protein sequence data sets.** *Nat Genet* 2001, **28**:281-285
 34. Tatusova TA, Karsch-Mizrachi I, Ostell JA: **Complete genomes in WWW Entrez: data representation and analysis.** *Bioinformatics* 1999, **15**:536-543
 35. Tatusov RL, Koonin EV, Lipman DJ: **A genomic perspective on protein families.** *Science* 1997, **278**:631-637
 36. Tatusov RL, Galperin MY, Natale DA, Koonin EV: **The COG database: a tool for genome-scale analysis of protein functions and evolution.** *Nucleic Acids Res* 2000, **28**:33-36
 37. Altschul SF, Madden TL, Schaffer AA, Zhang J, Zhang Z, Miller W, Lipman DJ: **Gapped BLAST and PSI-BLAST: a new generation of protein database search programs.** *Nucleic Acids Res* 1997, **25**:3389-3402
 38. Farris JS: **Phylogenetic analysis under Dollo's Law.** *Syst* 1977, **26**:77-88
 39. Swofford DL: *PAUP: phylogenetic analysis using parsimony (and other methods)*. Sunderland, MD: Sinauer; 1998
 40. Saitou N, Nei M: **The neighbor-joining method: a new method for reconstructing phylogenetic trees.** *Mol Biol Evol* 1987, **4**:406-425
 41. Grishin NV: **Estimation of the number of amino acid substitutions per site when the substitution rate varies among the sites.** *J. Mol. Evol* 1995, **41**:675-679
 42. Grishin NV: **Estimation of evolutionary distances from protein spatial structures.** *J Mol Evol* 1997, **45**:359-369
 43. Feng DF, Doolittle RF: **Converting amino acid alignment scores into measures of evolutionary time: a simulation study of various relationships.** *J Mol Evol* 1997, **44**:361-370
 44. Felsenstein J: **Inferring phylogenies from protein sequences by parsimony, distance, and likelihood methods.** *Methods Enzymol* 1996, **266**:418-427
 45. Notredame C, Higgins DG, Heringa J: **T-Coffee: A novel method for fast and accurate multiple sequence alignment.** *J Mol Biol* 2000, **302**:205-217
 46. Fitch WM, Margoliash E: **Construction of phylogenetic trees.** *Science* 1967, **155**:279-284
 47. Jones DT, Taylor WR, Thornton JM: **The rapid generation of mutation data matrices from protein sequences.** *Comput Appl Biosci* 1992, **8**:275-282
 48. Adachi J, Hasegawa M: *MOLPHY: Programs for Molecular Phylogenetics*. Tokyo: Institute of Statistical Mathematics; 1992
 49. Kishino H, Miyata T, Hasegawa M: **Maximum likelihood inference of protein phylogeny and the origin of chloroplasts.** *J. Mol. Evol* 1990, **31**:151-160
 50. Robinson DF, Foulds LR: **Comparison of phylogenetic trees.** *Math. Biosci* 1981, **53**:131-147
 51. Sneath PHA, Sokal RR: *Numerical Taxonomy*. San Francisco: W. H. Freeman; 1973

Publish with **BioMed Central** and every scientist can read your work free of charge

"BioMedcentral will be the most significant development for disseminating the results of biomedical research in our lifetime."

Paul Nurse, Director-General, Imperial Cancer Research Fund

Publish with **BMC** and your research papers will be:

- available free of charge to the entire biomedical community
- peer reviewed and published immediately upon acceptance
- cited in PubMed and archived on PubMed Central
- yours - you keep the copyright



BioMedcentral.com

Submit your manuscript here:

<http://www.biomedcentral.com/manuscript/>

editorial@biomedcentral.com